Measure synchronization in hybrid quantum–classical systems

Haibo Qiu(邱海波)[†], Yuanjie Dong(董远杰), Huangli Zhang(张黄莉), and Jing Tian(田静)

School of Science, Xi'an University of Posts and Telecommunications, Xi'an 710121, *China*

(Received 2 January 2022; revised manuscript received 26 March 2022; accepted manuscript online 20 April 2022)

Measure synchronization in hybrid quantum–classical systems is investigated in this paper. The dynamics of the classical subsystem is described by the Hamiltonian equations, while the dynamics of the quantum subsystem is governed by the Schrödinger equation. By increasing the coupling strength in between the quantum and classical subsystems, we reveal the existence of measure synchronization in coupled quantum–classical dynamics under energy conservation for the hybrid systems.

Keywords: measure synchronization, quantum measure synchronization, hybrid quantum–classical systems

PACS: 05.45.Mt, 64.60.–i, 03.75.Mn, 45.20.Jj **DOI:** 10.1088/1674-1056/ac685c

1. Introduction

Synchronization is ubiquitous in nature. It appears in ecosystems, physical systems, chemical systems, and even social behavior, etc.[1–4] Up to now, various types of synchronization have been found. e.g., phase synchronization,[5] complete synchronization,[6] lag synchronization,[7] projective synchronization,[8] and measure synchronization.[9] In the past decade, research interests of synchronization has been extended into quantum regime, and quantum synchronization has emerged as a new research field.[10–13] It has been shown that quantum synchronization is often related to quantum entanglement, or other kinds of quantum correlations. However, there are no general relations revealed yet, e.g., in some cases, the quantum synchronization can manifest only in the classical correlations rather than quantum correlations.[14]

In 1999, the concept of measure synchronization (MS) was proposed by Hampton and Zannett for coupled classical Hamiltonian systems.[9] They revealed a new type of synchronous behavior arising in coupled classical Hamiltonian systems, of which the coupled systems experience a synchronization transition, from a state in which the subsystems visit different phase space regions to a state in which their orbits cover the same region of the phase space with identical invariant measures. Up to now, classical MS behavior have been revealed in different model systems, i.e., ϕ_4 model,[15] Duffing model,[16] coupled bosonic Josephson junction[17,18] and more recently in non-dissipative Huygens' pendulum.[19] The classical concept of MS has been extended into quantum regime. We have revealed that quantum MS appears in coupled quantum many body systems, and quantum MS will manifest itself in a purely quantum mechanical way, i.e., collapses and revivals dynamics will get synchronized once the system reaching quantum MS.[20] More recently, quantum MS has also been found in a pair of Harper systems[21] and in between two scattering modes in Bose–Einstein condensates.[22]

Accompanied by the trend of extending classical concept of synchronization into quantum regime, there are also efforts in exploring intermediate regime in between classical and classical synchronization, i.e., quantum synchronization in semi-classical Kuramoto model,[23] and synchronization in quantum van de Pol oscillators.[24] Moreover, synchronization arising in coupled quantum–classical systems had been explored by one of the authors. Synchronous dynamics which termed as hybrid synchronization had been revealed based on the time correlation manifestations.[25] This kind of synchronization can be very strong, i.e., if the coupled classical system and quantum system have the exact correspondence in its initial conditions, the synchronization phenomenon can be as strong as complete synchronization.[25]

In this paper, we extend the investigation of measure synchronization into intermediate regime of quantum and classical dynamics, by exploring MS in a new scenario, of a system with coupled quantum–classical dynamics. This paper is organized as follows. Section 2 describes the coupled classical-quantum systems. Section 3 presents the results and an analysis of MS in the system. Finally, the results are summarized in Section 4.

2. Coupled quantum and classical Hamiltonian systems

In our previous investigation,[25] we have introduced a hybrid quantum–classical systems, which consists of one quantum Hamiltonian system $\hat{H}_a$ coupled with one classical Hamiltonian systems H_b. The coupled classical and quantum model systems can be written as $\hat{H} = \hat{H}_a + H_b + \hat{H}_{ab}$ with

$$\begin{aligned}\hat{H}_a \;=\; & -J_a(\hat{a}_L^{\dagger}\hat{a}_R + \hat{a}_L\hat{a}_R^{\dagger}) \\ & + \frac{U_a}{2}(\hat{n}_{a,L}(\hat{n}_{a,L}-1) + \hat{n}_{a,R}(\hat{n}_{a,R}-1)),\end{aligned}$$

[†]Corresponding author. E-mail: phyqiu@gmail.com

© 2022 Chinese Physical Society and IOP Publishing Ltd

$$\begin{aligned} H_b &= -2J_b\sqrt{n_{b,L}n_{b,R}}\cos\phi_b \\ &\quad + \frac{U_b}{2}\left(n_{b,L}(n_{b,L}-1)+n_{b,R}(n_{b,R}-1)\right), \\ \hat{H}_{ab} &= \frac{U_{ab}}{2}(\hat{n}_{a,L}-\hat{n}_{a,R})(N_b z_b), \end{aligned} \tag{1}$$

where $\hat{a}^{\dagger}_{L(R)}$ ($\hat{a}_{L(R)}$) are creation (annihilation) operators for the L or R modes of the quantum subsystem. $n_{b,L(R)}$ and ϕ_b are dynamical variables for classical subsystem which denote the particle number of L (R) mode and phase difference of b. The Hamiltonian includes tunneling terms, proportional to $J_{a(b)}$, which in absence of any interaction induce periodic Rabi oscillations of the populations between the states. The contact interaction translates into terms with strength proportional to U_a, U_b and U_{ab}, which gauge the aa, bb and ab contact interactions. Notice $\hat{H}_{ab}$ is the coupling term, which involve both classical and quantum variables, with U_{ab} denoting the coupling strength in between the quantum subsystem and the classical subsystem.

To study the coupled quantum–classical dynamics, we solve the following set of equations. For quantum subsystem, the dynamics is governed by the time dependent Schrödinger equation as

$$\mathrm{i}\partial_t|\Psi_a\rangle = \hat{H}(t)|\Psi_a\rangle. \tag{2}$$

For classical dynamics, we shall solve the Hamiltonian equations of motion,

$$\begin{aligned} \dot{z}_b &= -2J_b\sqrt{1-z_b^2}\sin\phi_b, \\ \dot{\phi}_b &= 2J_b\Lambda_b z_b + 2J_b\frac{z_b}{\sqrt{1-z_b^2}}\cos\phi_b + 2J_b\Lambda_{ab}\langle\hat{z}_a\rangle(t), \end{aligned} \tag{3}$$

where we have introduced the dimensionless ratios, $\Lambda_a \equiv N_a U_a/(2J_a)$, $\Lambda_b \equiv N_b U_b/(2J_b)$, and the new coefficient for coupling strength $\Lambda_{ab} \equiv N_a U_{ab}/(2J_b)$.

The time dependence of $\hat{H}$ stems from the time dependence of z_b, which can be seen as a classical parametric driving for the a subsystem. At the same time, we include the feedback effects of a on b through the last term of Eq. (3). It is worth to note that the effect of the quantum fluctuations of $\hat{z}_a$ is neglected in evaluating the dynamical evolution of ϕ_b, as we approximate $\hat{z}_a$ by its expectation value.

Considering the above mentioned reciprocal influence in between quantum and classical subsystems, we find that the solutions of Eqs. (2) and (3) are numerically conserve the total energy of the hybrid system in all the calculations reported in this paper. Conservation of the total energy also implies transfer of energy between the quantum and classical subsystems.

For numerical simulation of the quantum subsystem a, we employ the Crank–Nicolson method.[26] We choose Fock basis of the N_a+1 dimensional space, $|n_{a,L},n_{a,R}\rangle = \{|N_a,0\rangle,\ldots,|0,N_a\rangle\}$, and the most general a quantum state is written as

$$|\Psi_a\rangle = \sum_{k=0}^{N_a} c_k\,|k,N_a-k\rangle. \tag{4}$$

All many-body properties of the state are computed from the c_ks, e.g., the average population imbalance of the a subsystem reads

$$\langle\hat{z}_a\rangle = \sum_{k=0}^{N_a}|c_k|^2 z_{a,k} \tag{5}$$

with $z_{a,k} = (1-2k/N_a)$. The degree of condensation of a is given by its condensed fraction, i.e., the largest eigenvalue, n_1, of the single particle density matrix $\rho^a(t)$, $\rho^a_{ij}(t) = \frac{1}{N_a}\langle\Psi_a(t)|\hat{a}^{\dagger}_i\hat{a}_j|\Psi_a(t)\rangle$, $i,j = L,R$. The condensed fraction is also referred to as single-particle coherence. With this normalization, fully condensed a correspond to $n_1 = 1$ and $n_2 = 0$. In the following sections we discuss the time evolution of n_1 for different initial conditions and parameters.

3. Measure synchronization

As a special synchronization phenomenon in coupled Hamiltonian system, measure synchronization was originally defined only for coupled identical Hamiltonian systems.[9] Being identical, the only difference in between the coupled Hamiltonian systems are their initial conditions.[9,15–20] Even though for coupled quantum Hamiltonian and classical Hamiltonian systems, $\hat{H}_a$ and H_b, the two Hamiltonian systems are intrinsic different. Here we shall relax the requirement by setting the classical Hamiltonian system and quantum Hamiltonian system in exact correspondence except for their initial conditions. We set $N_a = N_b = 30$, $\Lambda_a = \Lambda_b = 0.1$, $J_a = J_b = 1$, and all the parameters with quantum–classical correspondence are the same. However, the initial conditions will be different for classical system and quantum system, here we choose initial conditions of quantum and classical systems without exact correspondence, i.e., we choose $\langle z_a\rangle = 0.6$, whereas $z_b = 0.1$, and $\langle\phi_a\rangle = \phi_b = 0$. Moreover, for quantum system, we will choose the initial state as a coherent state, which is the most classical-like quantum state. It reads

$$\begin{aligned} |\Psi_a(\theta_a,\phi_a)\rangle &= \sum_{k=0}^{N_a}\binom{N_a}{k}^{1/2}[\cos(\theta_a/2)]^k[\sin(\theta_a/2)]^{N_a-k} \\ &\quad\times \mathrm{e}^{\mathrm{i}(N_a-k)\phi_a}|k,N_a-k\rangle. \end{aligned} \tag{6}$$

Here $\cos(\theta_a) = \langle\hat{z}_a\rangle$, as mentioned above that we have chosen $\langle\hat{z}_a\rangle = 0.6$, so we need to set $\theta_a = \arccos(0.6)$ accordingly.

Our results reveal that measure synchronization (MS) occurs in coupled quantum–classical dynamics. The transition from non-MS states to MS states with increased coupling Λ_{ab} is shown in Figs. 1(a)–1(d). Due to the difficulty in defining a proper phase space for the quantum system in correspondence with the classical phase space, we adopt the method

employed in Ref. [20] to present a 3D phase space domain picture which have correspondence in between quantum and classical subsystems. Here we plot the evolution trajectory of pseudo-angular momentum for both quantum and classical subsystems, namely, $(j_x(t), j_y(t), j_z(t))$. The pseudo-angular momentum operators can readily be constructed from the creation and annihilation operators for quantum system,[27] $\hat{J}_x = (1/2)(\hat{a}_L^\dagger \hat{a}_R + \hat{a}_L \hat{a}_R^\dagger)$, $\hat{J}_y = 1/(2\mathrm{i})(\hat{a}_L^\dagger \hat{a}_R - \hat{a}_L \hat{a}_R^\dagger)$, and $\hat{J}_z = (1/2)(\hat{a}_L^\dagger \hat{a}_L - \hat{a}_R^\dagger \hat{a}_R)$. j_x, j_y and j_z are the average value of the pseudo-angular momentum operator, which are defined as following, $j_x = (2/N)\langle \hat{J}_x \rangle$, $j_y = (2/N)\langle \hat{J}_y \rangle$, and $j_z = (2/N)\langle \hat{J}_z \rangle$. In the same figure, we also plot $(j_x(t), j_y(t), j_z(t))$ of the classical Hamiltonian system. Here we derived $(j_x(t), j_y(t), j_z(t))$ from $(z_b(t), \phi_b(t))$ by the following transformations: $j_x = \sqrt{1 - z_b^2}\cos(\phi_b)$, $j_y = \sqrt{1 - z_b^2}\sin(\phi_b)$, and $j_z = z_b$.

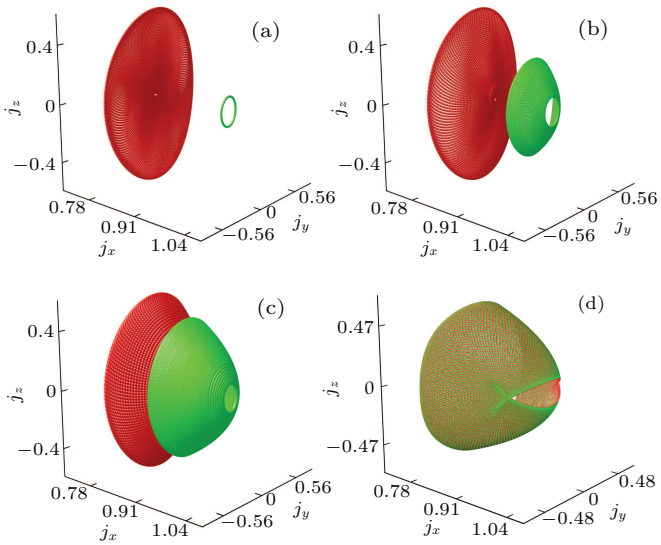


Fig. 1. Measure synchronization in hybrid quantum–classical systems characterized by the phase space domain covered during the evolution of each subsystem in the 3D phase space defined by pseudoangular momentum (j_x, j_y, j_z). (a) $\Lambda_{ab} = 0$; (b) $\Lambda_{ab} = 0.005$; (c) $\Lambda_{ab} = 0.01$; (d) $\Lambda_{ab} = 0.75$. Here $z_a(0) = 0.6, z_b(0) = 0.1, \theta_a(0) = \theta_b(0) = 0$, and $N_a = N_b = 30$.

For $\Lambda_{ab} = 0$, as shown in Fig. 1(a), there exists two distinctive phase space domains, one in green representing classical phase space domain and the other in red representing quantum phase space domain. It is worth noting that the classical phase space domain consists of a periodic orbit, meaning the classical dynamics is in periodic motion for $\Lambda_{ab} = 0$. However, for quantum dynamics, it is not a periodic motion.[20] As coupling strength Λ_{ab} increases, the two phase space domains will come closer, as shown in Figs. 1(b) and 1(c) for $\Lambda_{ab} = 0.005$ and 0.01, respectively. As coupling strength Λ_{ab} increases further, both phase space domains completely overlapped [e.g., Fig. 1(d) for Λ_{ab}=0.75], which indicates occurrence of MS.[9,20]

The transition process from non-MS to MS is shown in Fig. 2, in which we plot the average energies $\overline{E}_a/(N_a J_a)$ and $\overline{E}_b/(N_b J_b)$ as a function of the coupling Λ_{ab}. Here the red line represents $\overline{E}_a/(N_a J_a)$ of the quantum subsystem, and green line represents $\overline{E}_b/(N_b J_b)$ of classical subsystem. The average energies of the systems defined as

$$\overline{E}_{a(b)} = \frac{1}{T}\int_0^T E_{a(b)}(t)\,\mathrm{d}t, \tag{7}$$

where $E_a(t) = \langle \Psi(t)|\hat{H}_a|\Psi(t)\rangle$, and $E_b(t) = H_b$, with $|\Psi(t)\rangle$ the evolved quantum state.

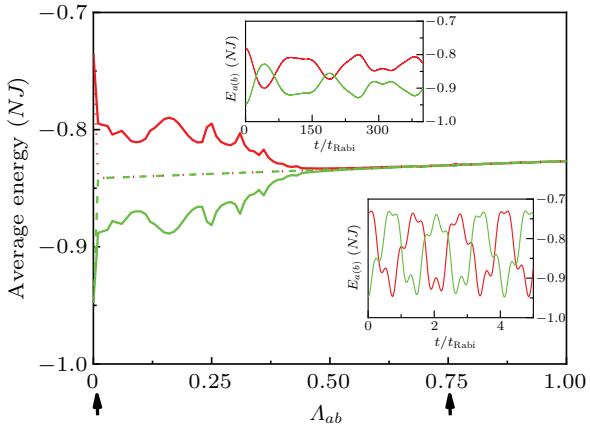


Fig. 2. Average energies $\overline{E}_{a(b)}/(N_{a(b)}J_{a(b)})$ versus Λ_{ab}, with $N = 30$. Red for average energy of the quantum system, and green for average energy of classical system. In the insets we depict $E_a(t)/(N_a J_a)$ and $E_b(t)/(N_b J_b)$ for two specific values of $\Lambda_{ab} = 0.01$ and $\Lambda_{ab} = 0.75$. The green and red dotted lines correspond to the classical prediction of Ref. [17].

The MS transition in coupled classical Hamiltonian systems is discontinuous as indicated by the average energy calculations.[15–17] This discontinuity allows us to define a critical point to characterize the MS transition. However, for the hybrid quantum–classical systems, the MS transition is continuous, which indicates the transition to MS is a crossover behavior. It is worth mentioning that MS transition in coupled quantum Hamiltonian systems is also a crossover behavior.[20] Besides, we have found that by increasing particle numbers $N = N_a = N_b$ while fixing other parameters and initial conditions, MS will occur at a smaller value of Λ_{ab} (e.g., for $N = 300$, and $\Lambda_c \approx 0.27$). And similar to MS transition in coupled classical Hamiltonian systems, extensive numerical simulations confirm that initial conditions have strong impact on MS transitions in hybrid quantum–classical systems. In general, more widely different choice of initial conditions for the two subsystems result in a larger value of Λ_c for the onset of MS.

The physical mechanism behind MS transition in coupled quantum–classical dynamics is revealed in Fig. 3. The condensed fraction n_1 versus time for three different coupling strength are presented in Fig. 3(a), with $\Lambda_{ab} = 0, 0.01$, and 0.75. We note that $n_1(t)$ will be closer to its initial value 1, as coupled strength increased. At initial time, $n_1 = 1$ corresponds to the initial quantum state as a coherent state,

which is the most classical-like of all quantum states. So in time evolution, $n_1(t) \approx 1$ means quantum evolution is essentially coherent. The results indicate that as coupling strength increases, the quantum subsystem will behave more classically. Figure 3(b) shows the dispersion of population imbalance $\sigma_z^2 = \langle \hat{z}_a^2 \rangle - \langle \hat{z}_a \rangle^2$ versus time for different coupling strength. It is found that with increased coupling strength, the dispersion is suppressed gradually, and it is much more closer to 0 as the coupled quantum–classical dynamics reaches MS. This indicates that as coupling strength in between the quantum subsystem and classical subsystem increases, the quantum fluctuations (as revealed by dispersion) for the quantum subsystem will be greatly suppressed. In summary, we find that the reason behind the appearance of MS in coupled quantum–classical dynamics is the fact that the quantum system will become more classical-like as a result of the coupling effects in between the quantum and classical systems.

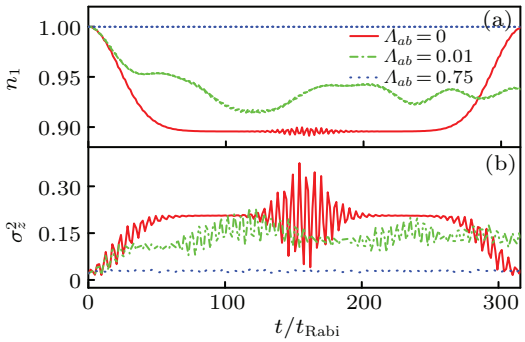


Fig. 3. Coupling effects on evolution of two relevant quantum properties. Panels (a) and (b) depict the dispersion of the condensed fraction n_1 and the population imbalance σ_z^2, respectively. $\Lambda_{ab} = 0$, 0.01, and 0.75 for both panels. All other parameters are the same as in Fig. 1.

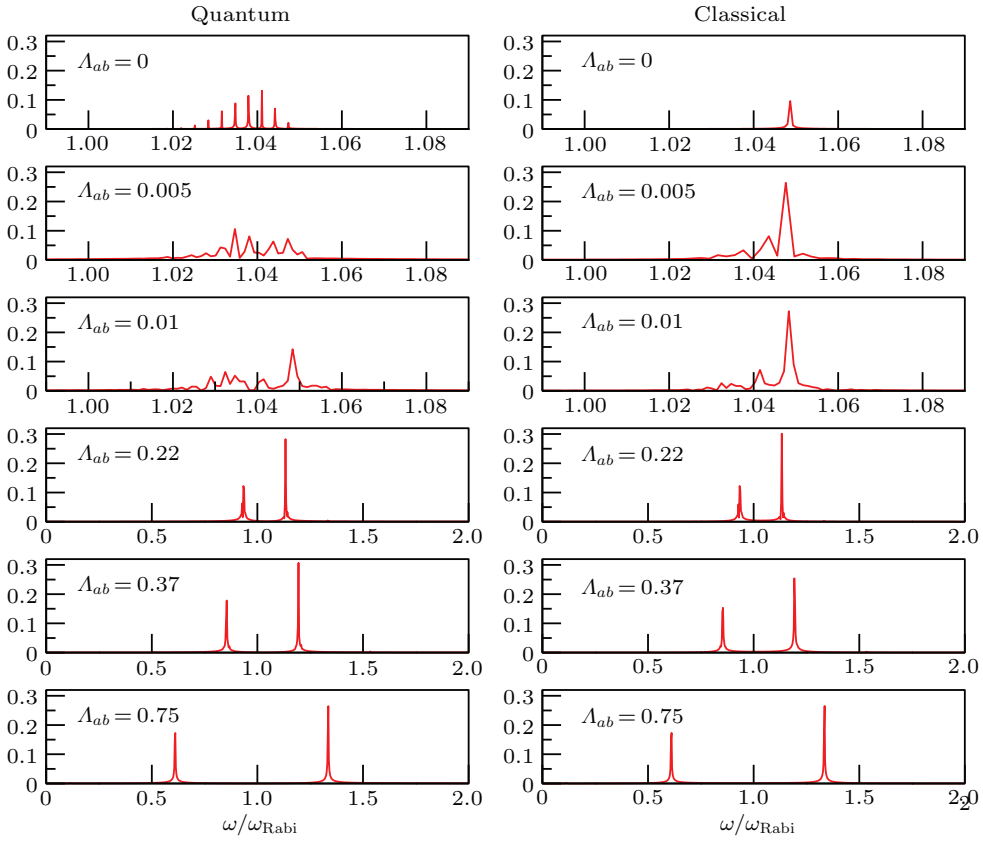


Fig. 4. Absolute value of the frequency spectrum $z(\omega)$ (Fourier transform of the average population imbalances), for different values of the coupling strength $\Lambda_{ab} = 0/0.005/0.01/0.22/0.37/0.75$. The frequency spectrum of the quantum result, $\langle \hat{z}_a \rangle(\omega)$ is given in the left panels. $z_b(\omega)$ is depicted in the right panels. The frequency spectra are obtained from time series up to $T_{\rm Max} = 732 t_{\rm Rabi}$.

To analyze time correlated dynamics behind measure synchronization in hybrid quantum–classical systems, the Fourier decomposition of the evolution of the population imbalance is presented in Fig. 5. The frequency spectra of these signals are for different values of Λ_{ab}. In the uncoupled case the quantum signal is found to have several peaks around the frequency $\omega \simeq 1.04\omega_{\rm Rabi}$. The different peaks reflect the multi-frequency nature of quantum dynamics. In contrast, the classical signal is found to have only one peak, as a result of period motion of $z_b(t)$. As we couple the two subsystems, the spread in the a subsystem disappears and two prominent frequencies appear both for a and b. For $\Lambda_{ab} = 0.22$ and $\Lambda_{ab} = 0.37$ (fourth and fifth row) the Fourier decompositions of both signals are very similar, showing two large peaks at the same frequencies for the two signals, however, a closer scrutiny show that the amplitudes of the two peaks are a bit different. Keeping increasing the coupling strength, for $\Lambda_{ab} = 0.75$, we have the same Fourier structure in both cases, signaling the appearance of

measure synchronization. This feature is shared by measure synchronization in two coupled classical Hamiltonian system, where two subsystems get frequency-locked with very few frequencies being involved.[19] In contrast, for quantum measure synchronization, we have found that the frequency locking involves multiple frequencies.

At last, we investigate the many body effects on the coupled quantum–classical dynamics. Here we fix the coupling strength $\Lambda_{ab} = 0.4$, and only change particle numbers, with $N = 6/10/20/80$. The initial conditions are the same as in Fig. 1. It is found that with increasing particle numbers, the dispersion will be suppressed as a result, as shown in Fig. 4(a). Meanwhile, the condensed fraction will be more close to its initial value as particle number increases. Compared with Fig. 3, we notice the increased coupling strength and increased particle numbers have similar effects. That is, as commented above, to make the quantum subsystem more classical-like. The two results shown in here are quite natural considering the effects of particle number on quantum many body dynamics of $\hat{H}_a$ all alone. As $N \to \infty$, $\langle\Psi|\hat{H}_a|\Psi\rangle$ can approach its "classical" limit, which in the quantum–classical correspondence, is H_b.

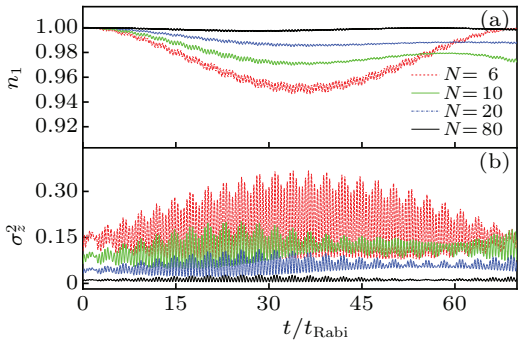


Fig. 5. Many body effects on evolution of two relevant quantum properties. Panels (a) and (b) depict the condensed fraction n_1, and the dispersion of the population imbalance σ_z^2, respectively. Particle numbers $N = 6$, 10, 20 and 80 for both panels. The coupling strength $\Lambda = 0.4$ is fixed. All other parameters are the same as in Fig. 1.

In the end, we have shown how the MS has emerged in the coupled quantum–classical dynamics. As a comparison, hybrid synchronization (HS) can also exist in the same model system.[25] The differences between these two synchronization concepts lie in two aspects. Firstly, MS is a synchronization in the sense of spatial coincidence,[28] and it is a special synchronization characterized by phase space domain with invariant measure.[9] On the other hand, HS is a synchronization in the sense of time coincidence, and it is a general term for synchronization characterized by its strong time correlation in coupled quantum–classical dynamics. The time correlations can be as strong as complete synchronization, while in term of time correlation, MS is much weaker compared with complete synchronization. Secondly, there are dramatic difference in setting the initial conditions and parameters for hybrid synchronization and measure synchronization. For hybrid synchronization, we had required the quantum subsystem and classical subsystem to have the initial conditions with exact correspondence,[25] while for measure synchronization, the initial conditions can not have exact correspondence, and must be different.

4. Conclusion

In this paper, we have introduced the concept of measure synchronization in hybrid quantum–classical systems. It is found that MS can be induced by increasing the coupling strength in the hybrid quantum–classical system. However, the MS transition being found is a crossover behavior rather than a critical behavior. Similar feature also appears in quantum measure synchronization.[20] For the physical reason behind MS, we have revealed that as coupling strength in the hybrid quantum–classical systems increase, the quantum subsystem will behave more classical-like. And this effects leads to measure synchronization mimicking measure synchronization in coupled classical Hamiltonian systems. It is further shown that, with coupling strength increasing, the frequency spectra of the MS states share similar results as classical MS states.

Acknowledgements

Project supported by the National Natural Science Foundation of China (Grant No. 11402199), the Natural Science Foundation of Shaanxi Province, China (Grant Nos. 2022JM-004 and 2018JM1050), and the Education Department Foundation of Shaanxi Province, China (Grant No. 14JK1676).

References

[1] Kuramoto Y 1984 *Chemical Oscillations, Waves and Turbulence* (Berlin: Springer)
[2] Néda Z, Ravasz E, Brechet Y, Vicsek T and Barabási A L 2000 *Nature* **403** 849
[3] Arenas A, Díaz-Guilera A, Kurths J, Moreno Y and Zhou C 2008 *Phys. Rep.* **469** 93
[4] Pikovsky A, Rosenblum M and Kurths J 2003 *Synchronization: A Universal Concept in Nonlinear Sciences* (Cambridge: Cambridge University Press)
[5] Rosenblum M G, Pikovsky A S and Kurths J 1996 *Phys. Rev. Lett.* **76** 1704
[6] Pecora L M and Carroll T L 1990 *Phys. Rev. Lett.* **64** 821
[7] Rosenblum M G, Pikovsky A S and Kurths J 1997 *Phys. Rev. Lett.* **78** 4193
[8] Mainieri R and Rehacek J 1999 *Phys. Rev. Lett.* **82** 3042
[9] Hampton A and Zanette D H 1999 *Phys. Rev. Lett.* **83** 2179
[10] Zhirov O V and Shepelyansky D L 2006 *Eur. Phys. J. D* **38** 375
[11] Lee T E and Sadeghpour H R 2013 *Phys. Rev. Lett.* **111** 234101
[12] Galve F, Giorgi G L and Zambrini R 2017 *Lectures on General Quantum Correlations and Their Applications* (Berlin: Springer) pp. 393–420

[13] Zhou K J, Zou J, Xu B M, Li L and Shao B 2021 *Commun. Theor. Phys.* **73** 105101
[14] Lörch N, Amitai E, Nunnenkamp A and Bruder C 2016 *Phys. Rev. Lett.* **117** 073601
[15] Wang X, Zhan M, Lai C H and Gang H 2003 *Phys. Rev. E.* **67** 066215
[16] Vincent U E 2005 *New J. Phys.* **7** 209
[17] Tian J, Qiu H B, Wang G F, Chen Y and Fu L B 2013 *Phys. Rev. E* **88** 032906
[18] Tian J, Wang Y F and Qiu H B 2020 *Commun. Theor. Phys.* **72** 055701
[19] Tian J, Li B, Liu T and Qiu H B 2019 *Chaos* **29** 093131
[20] Qiu H B, Juliá-Díaz B, García-March M A and Polls A 2014 *Phys. Rev. A* **90** 033603
[21] Sur S and Ghosh A 2019 *Phys. Lett. A* **384** 126176
[22] Zhang L, Xu X T and Zhang W P 2020 *Eur. Phys. J. Plus* **135** 202
[23] Hermoso de Mendoza I, Pachón L A, Gómez-Gardeñes J and Zueco D 2014 *Phys. Rev. E* **90** 052904
[24] Walter S, Nunnenkamp A and Bruder C 2014 *Phys. Rev. Lett.* **112** 094102
[25] Qiu H B, Zambrini R, Polls A, Martorell J and Juliá-Díaz B 2015 *Phys. Rev. A* **92** 043619
[26] Press W H, Flannery B P, Teukolsky S A and Vetterling W T 1988 *Numerical Recipes in C* (Cambridge: Cambridge University Press)
[27] Leggett A J 2001 *Rev. Mod. Phys.* **73** 307
[28] Qiu H B, Tian J and Fu L B 2010 *Phys. Rev. A* **81** 043613